Published in final edited form as:
J Neurosci Methods. 2007 July 30; 163(2): 213–225.

Anterograde Tracing Method using DiI to Label Vagal Innervation of the Embryonic and Early Postnatal Mouse Gastrointestinal Tract

Michelle C. Murphy and **Edward A. Fox**
Behavioral Neurogenetics Laboratory, Department of Psychological Sciences, Purdue University, West Lafayette, IN, USA 47907

Abstract

The mouse is an extremely valuable model for studying vagal development in relation to strain differences, genetic variation, gene manipulations, or pharmacological manipulations. Therefore, a method using 1, 1′-dioctadecyl-3,3,3′,3′-tetramethylindocarbocyanine perchlorate (DiI) was developed for labeling vagal innervation of the gastrointestinal (GI) tract in embryonic and postnatal mice. DiI labeling was adapted and optimized for this purpose by varying several facets of the method. For example, insertion and crushing of DiI crystals into the nerve led to faster DiI diffusion along vagal axons and diffusion over longer distances as compared with piercing the nerve with a micropipette tip coated with dried DiI oil. Moreover, inclusion of EDTA in the fixative reduced leakage of DiI out of nerve fibers that occurred with long incubations. Also, mounting labeled tissue in PBS was superior to glycerol with n-propyl gallate, which resulted in reduced clarity of DiI labeling that may have been due to DiI leaking out of fibers. Optical sectioning of flattened wholemounts permitted examination of individual tissue layers of the GI tract wall. This procedure aided identification of nerve ending types because in most instances each type innervates a different tissue layer. Between embryonic day 12.5 and postnatal day 8, growth of axons into the GI tract, formation and patterning of fiber bundles in the myenteric plexus and early formation of putative afferent and efferent nerve terminals were observed. Thus, the DiI tracing method developed here has opened up a window for investigation during an important phase of vagal development.

Keywords

Autonomic; Stomach innervation; Intraganglionic laminar ending; Intramuscular array; Mechanoreceptor; Vagus nerve; Visceral Afferents; Visceral Efferents

1. Introduction

The sensory division of the vagus nerve informs the brain about GI tract activity and regulates vago-vagal digestive reflexes important for GI tract function, whereas vagal efferent preganglionic neurons comprise the final common pathway that integrates sensory and CNS inputs to regulate digestive functions (Travagli et al., 2006). Despite the importance of vagal innervation of the GI tract, many aspects of its structural and functional organization are poorly

Correspondence: Edward A. Fox, Department of Psychological Sciences, 703 Third Street, Purdue University, West Lafayette, IN 47907, Telephone: 765-494-5917, Fax: 765-496-1264, E-mail: au_gc@psych.purdue.edu

understood. Similarly, knowledge of the development of this innervation, which could help elucidate its organization, is lacking.

The slow progress in studying vagus nerve development has mainly resulted from an inability to apply commonly employed nerve labeling techniques selectively and non-invasively to the vagus nerve in embryos and neonates. For example, the method that labels nerve fibers and terminals using immunohistochemical (IHC) staining of neuron-specific antigens has been useful in many peripheral neural systems, including taste and somatosensory pathways (Fundin et al., 1997;Nosrat et al., 1997). However, this method has not been feasible for the vagus because it also labels the sympathetic, spinal visceral afferent and enteric nervous systems, which innervate the same GI tissues as the vagus (Hayashi et al., 1982;Richards and Sugarbaker, 1995;Schafer et al., 1998), and the co-extensive elements of these systems typically cannot be distinguished. A second labeling strategy that could overcome this limitation involves the use of IHC markers selective for developing vagal innervation. One of the best candidates is $P2X_3$ receptor immunoreactivity, which labels vagal axons, intraganglionic laminar endings (IGLEs) and intramuscular arrays (IMAs) in the developing rat stomach wall, but unfortunately enteric nervous system elements are also labeled (Xiang and Burnstock, 2004). Additionally, there are two IHC markers for IGLEs, but they have only been characterized in the adult mouse (vesicular glutamate transporter 2, $P2X_2$ receptor; Castelucci et al., 2003;Raab and Neuhuber, 2005). The third strategy involving the use of neural tracers, including wheat-germ agglutinin-horseradish peroxidase (WGA-HRP) and dextran conjugates (Fox et al., 2000;Neuhuber, 1987;Phillips et al., 1997;Wang and Powley, 2000), which has been valuable for labeling the vagus in the adult rodent, is not practical for labeling the embryonic or neonatal vagus because the associated tissue damage could alter structural or temporal aspects of its differentiation (Haworth et al., 1998;Mitani, 1989).

One approach with the potential to address these obstacles is post-mortem tracing with DiI. DiI nerve tracing is ideal for labeling neurons and tracing axons and nerve terminals in postmortem tissue as it diffuses readily through aldehyde-fixed plasma membranes (Godement et al., 1987). This eliminates the need for surgical or anesthesia procedures (Lukas et al., 1998), obviating the potential effects of damage inflicted with the use of other anterograde tracers that could alter normal neural development (e.g., WGA-HRP). It also makes possible studies of the effects of mutations of developmental genes that are lethal perinatally, whereas tracers such as WGA-HRP that require active transport are not feasible in this situation because sufficient time for anterograde transport is lacking. Further, DiI is compatible with the counterstaining and IHC techniques employed for visualizing tissue elements that interact with vagal terminals (Elberger and Honig, 1990;Lukas et al., 1998).

The potential of the DiI method for labeling developing vagal GI tract innervation derives from its successful use for studying the development of several other peripheral neural pathways. For example, DiI has been used to label nerve cells, axons and terminals as they first appear during development and to characterize their location, relative density and morphology at different stages of development, as well as changes in these features that result from gene manipulations (Fritzsch et al., 1997;Krimm et al., 2001;Mirnics and Koerber, 1995;Rontal and Echteler, 2003;Wang and Scott, 1999). Post-mortem nerve tracing with DiI has been utilized successfully in the rat to characterize the development of vagal preganglionic neurons that innervate the gut, and vagal sensory innervation of the nucleus of the solitary tract that originates in the gut, or in other visceral organs and cranial nerves (Rinaman and Levitt, 1993;Zhang and Ashwell, 2001). However, to our knowledge, Sang and Young (1998) have provided the only report of selective labeling of developing vagus nerve terminals in the embryonic GI tract. They demonstrated that anterograde DiI tracing could label vagal fibers and terminals innervating the esophagus at several stages between embryonic day (E)12-E18 in mice. Importantly, this work illustrated the potential of the DiI method, which if further

developed could be valuable for study of the development of vagal innervation in other GI organs.

Thus, our goal in the present study was to adapt and optimize anterograde nerve tracing with DiI to selectively label the developing vagal innervation of the GI tract wall. The mouse was utilized to take advantage of the potential for manipulation of genes involved in neural development, and to capitalize on the shorter distance DiI must diffuse to label organ innervation as compared with the distances required in other commonly studied rodents such as the rat and guinea pig.

2. Materials and Methods

2.1 Embryos and postnatal mice

Mice of the 129SvJae strain (or mice with a predominantly C57Bl/6 background, Experiment 3) from our colony were maintained at 22°C on a 12:12 light/dark cycle with lights on at 0500 and off at 1700. Mice had ad libitum access to tap water and chow pellets (Laboratory Rodent Diet 5001, PMI Nutrition International, Inc., St. Louis, Missouri). All procedures were conducted in accordance with Principles of Laboratory Animal Care (NIH publication No. 86-23, revised 1985) and American Association for Accreditation of Laboratory Animal Care guidelines and were approved by the Purdue University Animal Care and Use Committee.

To acquire embryos at specific ages, males were placed with females for 20 min between 2000 and 2100 hr and monitored to ensure copulation occurred. The following day at 1200 h was designated E0.5. Postnatal mice were obtained from a subset of these matings and the day of birth was defined as postnatal day (P)0.

2.2 Harvesting and fixation of embryos and neonates

Pregnant mice were euthanized by cervical dislocation, the uterus was removed and placed in chilled 0.1M sodium phosphate buffered saline (PBS) on ice, embryos were dissected free and their abdominal organs exposed. Next, embryos were transferred to fresh 4% paraformaldehyde (and 0.1% ethylene-diamine tetraacetate (EDTA) for some specimens) for 3 d at 4°C, and then to PBS, 0.5% sodium azide and stored at 4°C. Alternatively, after birth mice were given a lethal dose of methohexital sodium (Brevital Sodium, Eli Lilly, Indianapolis, Indiana; 100 mg/kg i.p.) and perfused transcardially with saline at 40°C for 5 min followed by ice-cold 4% paraformaldehyde (and 0.1% EDTA for some specimens) for 30 min. Next, mice were stored in the same fixative for 3 d at 4°C and then transferred to PBS, 0.5% sodium azide and stored at 4°C.

2.3 Imaging of DiI-labeled tissues

DiI in crystal (perchlorate; D3911, Molecular Probes, Eugene, Oregon) or oil (methanesulfate; D3886, Molecular Probes) form was employed as a postmortem nerve tracer for selectively labeling the division of the developing vagus nerve that supplies the GI tract. DiI is a fluorescent lipophilic dye that diffuses along the lipid bilayer of membranes, traveling laterally. Transfer between membranes is usually negligible (Hofmann and Bleckmann, 1999;Honig and Hume, 1986). DiI emits a distinct red fluorescence at 565 nm that was examined using a Nikon E1000 fluorescence microscope and standard rhodamine optical filters (TRITC filter cube; Tokyo, Japan). Also, vagal nerve fibers and terminals labeled with DiI were scanned with a multi-photon confocal microscope (Radiance 2100 MP Rainbow with green helium-neon laser, 543nm; Bio Rad, Hemel Hempstead, England) combined with a TE2000 inverted microscope (Nikon, Tokyo, Japan) and motorized stage (Marzhauser, Weizlar, Germany), and run with LaserSharp 2000 software system (Bio-Rad). Image processing and three-dimensional reconstructions were done using Confocal Assistant software (v4.02, Todd Brelje, University

of Minnesota). Alternatively, DiI-labeled neural elements were scanned with an Olympus BX-DSU spinning disk confocal microscope and processing of three-dimensional image data was performed using Slidebook software (v.4.1, Intelligent Imaging Innovations, USA).

2.4 Experiment 1. Application of dried DiI oil using a glass micropipette tip

One of the commonly used DiI methods involves application of DiI crystals. Such application to nerves can result in redistribution of DiI from the application site to other tissues (Lukas et al., 1998). Therefore, to maximize transfer of DiI to nerve fibers while minimizing the potential for its redistribution, DiI oil was dried on a micropipette tip (inner tip diameter = 25 μm) and applied to the vagus nerve. Micropipettes were prepared by pulling borosilicate glass capillaries (M1B120F-4, World Precision Instruments, Germany) using a glass capillary puller (PE-2, Narishige- Scientific Instruments Laboratory, Japan). The micropipette tips were then dipped in DiI oil, which was allowed to dry overnight in the dark at 4°C.

2.4.1 Experimental protocol—After perfusion and fixation, the liver was carefully removed under a dissecting microscope to visualize the stomach and the esophagus with associated vagal trunks and branches. DiI was applied to the vagus nerve using a stereotax to guide the DiI-coated micropipette tip through the nerve, puncturing it several times until as much of the DiI as possible was transferred to the nerve. DiI was inserted in this manner into the anterior trunk of the abdominal vagus as it courses along the esophagus, immediately anterior to the bifurcation of the hepatic and gastric branches (E16.5, n=4; P0, n=13; P1, n=3). This site was optimal in being close enough to the stomach to minimize the necessary DiI diffusion distance, yet far enough from the stomach to curtail non-specific spread of DiI from the insertion site to this organ. Also, targeting DiI insertion to this site was practical because it is a readily identifiable anatomical landmark, and thus was used to place the DiI in a similar locus in each animal. Mice were then placed in PBS, 0.5% sodium azide at 37°C for 1–7 weeks.

The anterior vagal trunk and gastric branch were examined every 2–3 days to track the distance DiI traveled from the application site. For this purpose, the stomach and esophagus with the attached vagal trunks were dissected free from the embryo, temporarily mounted in PBS, and examined with fluorescence microscopy. Postnatal stomachs were treated similarly except that prior to mounting they were opened along the greater curvature, milk was removed, the stomach cavity was rinsed with PBS. The distance DiI traveled from the application site within the anterior vagal trunk and gastric branch was measured using an eyepiece grid (0.225 × 0.225 mm) at a total magnification of 400X. Because the front edge of the diffusing DiI gradually faded, it was difficult to identify precisely. Therefore, the measurement taken was at half the distance between the approximated front edge where it faded out and the approximate front edge of bright labeling in the nerve trunk, where fading began. After measurement the tissue was returned to incubation in fresh PBS, 0.5% sodium azide at 37°C.

2.5 Experiment 2A: Effect of increasing the amount of DiI applied to the vagus nerve

Since the method used in Experiment 1 was not effective at labeling vagal innervation of the stomach wall (see Results), we examined two different methods of augmenting the amount of DiI applied: (1) increasing the amount of DiI that was dried on micropipette tips, or (2) inserting DiI crystals directly into the nerve.

The amount of DiI dried onto each micropipette tip was increased by performing the coating and drying process described in Experiment 1 twice for each tip. This DiI-coated micropipette tip was then inserted in the nerve as described for Experiment 1 (P0; n=17). Alternatively, after exposing the anterior vagal trunk, one DiI crystal was inserted into the nerve and then crushed into the nerve fibers using #5 straight tip fine forceps (Dumont, Switzerland) at the same site described in Experiment 1 (P0; n=12). Sheets of tissue paper (1 inch sq) that had been twisted

were used to aid in restricting spread of DiI from the application site by helping to keep tissues near the application area dry and free of DiI fragments created during crushing.

In Experiment 1, the long durations required for DiI diffusion along vagal axons to reach the stomach were associated with a gradual decline in the clarity of the DiI labeling of nerve fibers, suggesting that DiI was leaking out of them (see Results). Hofmann and Bleckmann (1999) found that incorporation of EDTA into the fixative contributed to retarding the diffusion of DiI out of membranes, thereby increasing the specificity of DiI labeling and preventing transneuronal labeling. Therefore, we added 0.1% EDTA to the fixative. Tissues were examined to determine the distance DiI had diffused along the vagus nerve as described in Experiment 1 except that they were first examined 1 wk after DiI insertion and subsequently every 0.5 wk.

2.5.1 Experiment 2B: Effect of mounting medium on DiI labeling Some stomachs from Experiment 2A were mounted in glycerol with n-propyl gallate to reduce fading of DiI fluorescence (Giloh and Sedat, 1982). Surprisingly, there was an increase in red fluorescence in the background and reduced clarity of DiI labeled nerve fibers, suggesting DiI may have leaked out of these fibers (see Results). In contrast, DiI labeling of vagal fibers was clearly visualized when temporarily mounted in PBS to assess DiI diffusion in Experiment 1. Therefore, the effects of permanent mounting in these media were directly compared. DiI crystals were applied as in Experiment 2A in P0 mice and DiI was permitted to diffuse for 3 wk prior to mounting. Stomachs, along with the pylorus, the initial portion of the duodenum and the abdominal esophagus, were prepared as wholemounts and either cleared with gentle agitation in glycerol (70% in PBS, 30 min) and mounted in 70% glycerol, 5% n-propyl gallate (n=3), or mounted directly in PBS (n=2), coverslipped and sealed with clear nail polish (AM Products, NJ, USA) and then examined for DiI labeling. All other procedures were the same as described for Experiment 2A.

2.5.2 Experiment 2C: Verification of vagal origin of labeled axons and nerve terminals To ensure that DiI-labeled fibers and terminals were vagal in origin, the anterior vagal gastric branch was cut with fine scissors between the DiI application site and the stomach immediately after DiI application to the anterior vagal trunk (E16.5, n=2; P0, n=5; P3, n=1). After 3 wk incubation the stomachs were mounted in PBS and examined for the presence of DiI-labeled axons. Other methods were the same as for DiI crystal application in Experiment 2A.

2.6 Experiment 3: Characterization of DiI-labeled axons and terminal specializations

The vagal innervation supplying the stomach wall was labeled utilizing the optimal conditions determined in Experiments 1 and 2, which included DiI crystal application, preservation of labeled tissues with fixative that included EDTA, and mounting DiI-labeled tissues in PBS. Qualitative observations were made on the development of axons, fiber bundles and nerve terminal specializations in 129SvJae embryos (E12.5, n=8; E13.5, n=6; E14.5, n=3; E15.5, n=4; E16.5, n=7; E17.5, n=3), 129SvJae postnatal mice (P0, n=16; P1, n=6; P2, n=8; P3, n=13; P4, n=4; P5, n=4; P8, n=4; and P10, n=4), and C57Bl/6 P0 mice (n=6).

2.6.1 Criteria for including specimens in analysis—Specimens were first examined using a fluorescence microscope to assess several criteria for sufficient labeling: (1) A significant proportion of vagal fibers and terminals in all stomach wall compartments were labeled with DiI, and this labeling extended distally as far as the greater curvature and pylorus. (2) DiI labeling remained stable during diffusion and imaging, i.e. DiI did not leak out of vagal fibers. (3) DiI did not redistribute from the injection site to produce non-specific labeling. Five

percent of the specimens exhibited evidence of incomplete DiI-labeling, none had DiI leakage, and 20% showed DiI redistribution. None of these specimens were examined further.

2.6.2 Criteria for identification of afferent and efferent terminal specializations

—Published criteria for identifying mature forms of IGLEs, IMAs and efferent terminals were utilized here to identify their putative immature forms or precursors based on the assumption they would exhibit unique features of the mature forms, although these features (e.g., nerve terminal components) might be smaller in size, less numerous, or less dense. The criteria for counting an ending as a mature IGLE are that it consists of (1) a laminar (2) aggregate of fine terminal puncta (3) within the neuropil of a myenteric ganglion (4) covering all or part of the ganglion (Neuhuber, 1987;Neuhuber et al., 1995;Rodrigo et al., 1982;Rodrigo et al., 1975). The criteria for counting an ending as a mature IMA are that it consists of (1) an array of parallel axonal telodendria (2) in close proximity, (3) interconnected by bridging axonal elements and (4) located in either the longitudinal or circular muscle layer (Berthoud and Powley, 1992;Fox et al., 2000;Wang and Powley, 2000). Finally, the criteria for counting an ending as a mature efferent terminal are that it consists of (1) a network of characteristic rings of fiber arborizations and terminal complexes (2) circling the myenteric neurons (3) within the myenteric ganglia (Holst et al., 1997;Kirchgessner and Gershon, 1989;Phillips et al., 2003). Additionally, an identification process that combined optical sectioning of confocal imaging with the simple planar geometry of the stomach wall layers was developed that aided assessment of these criteria by permitting determination of the tissue layer innervated by each labeled ending. Examining the stomach wall as a wholemount resulted in horizontal orientation of each of its tissue layers and of the optical sections. Thus, as the optical sections progressed through the z-axis, which was perpendicular to these tissue layers, images were captured successively from top to bottom through the longitudinal muscle layer, the myenteric plexus, the circular muscle layer, the submucosa and the mucosa.

2.7 Experiment 4: Adaptation of DiI labeling protocol to innervation of the esophagus and intestine

The feasibility of adapting the DiI method employed in Experiment 3 for studying development of vagal innervation of the other major gastrointestinal organs, the esophagus and intestine was assessed. For labeling the vagal innervation of the esophagus wall, DiI crystals were applied either bilaterally to the cervical vagus nerves at locations between the nodose ganglion and the most anterior esophageal vagal branches, or to the anterior abdominal trunk immediately anterior to the bifurcation of the anterior gastric and hepatic branches (E15.5, n=4; E18.5, n=6; P0, n=12). For labeling the vagal innervation of the intestine wall DiI was applied to the anterior abdominal trunk immediately anterior to the bifurcation of the anterior gastric and hepatic branches, as well as an analogous site within the posterior vagal trunk immediately anterior to the bifurcation of the celiac and gastric branches (E15.5, n=4; E18.5, n=4; P0, n=8), or to more distal locations along the celiac branches (E18.5, n=2; P0, n=5). After DiI incubation for 4–6 wk, the esophagus was dissected free, cut along the tracheal attachment, and wholemounted mucosal side facing down. The proximal end of the duodenum was separated from the pylorus and its distal end separated from the remaining intestine at the duodenojejunal flexure and wholemounted in a consistent orientation with the mesenteric attachment to one side. The remainder of the intestine was cut into 1 cm segments and mounted in a similar manner.

3. Results

3.1 Experiment 1. Application of DiI oil dried onto a glass micropipette tip

Incubation periods of 4–7 weeks resulted in limited diffusion of DiI as far as 2–3.5 mm from the injection site, which was not sufficient to label vagal fibers throughout the stomach wall, nor to label them as far as the greater curvature (diffusion distance from DiI placement site

toward greater curvature of stomach, mean ± SEM: E16.5: 2.5 ± 0 mm; P0:, 1.35 ± 1.1 mm; P1:, 2 ± 0.5 mm). Also, after lengthy incubation of 4–5 wk or longer DiI appeared to leak out of nerve fibers into the media and adjacent muscle wall, greatly reducing the clarity of the labeled fibers (Fig. 1A).

3.2 Experiment 2A. Effect of increasing the amount of DiI applied to the vagus nerve

Although not directly compared in the same experiment, increasing the amount of dried DiI oil applied to the vagus in the present experiment did appear to improve labeling as compared to Experiment 1. DiI labeling of nerve fibers now extended along the stomach wall as far as the greater curvature. An even greater improvement in labeling occurred with application of DiI in crystal form to the vagal nerve trunk as the rate of DiI diffusion increased and labeling of stomach wall innervation was more complete (Fig. 1B). In particular, compared with DiI oil, crystal DiI application labeled a greater number of nerve fibers, which were distributed throughout the organ wall, and increased numbers of labeled fibers reached the greater curvature. Further, the time required for DiI diffusion to label nerve fibers extending to the greater curvature was on average approximately 1 wk less for DiI crystals than for the DiI oil (DiI crystal, 3.04 ± 0.21 wk; DiI oil, 3.82 ± 0.16 wk).

3.2.1 Experiment 2B. Effect of mounting medium on DiI labeling—Immediately after clearing in 70% glycerol and mounting in 70% glycerol with 5% n-propyl gallate, DiI labeled fibers in the stomach wall were distinct, but within a few hours images of the stomach wall exhibited an increase in red fluorescence in the background as DiI diffused into the mounting medium and surrounding tissue so that labeled fibers were no longer clear or distinct (Fig. 1C). In contrast, specimens mounted directly in PBS resulted in the background and the stomach wall remaining clear over the period of examination, permitting better visualization of distinct fibers and terminals (Fig. 1D).

3.2.2 Experiment 2C. Verification of vagal origin of labeled axons and nerve terminals—Three weeks after DiI application and sectioning of the vagus no DiI labeled fibers were detected in the stomach wall of one of the E16.5 embryos and three of the P0 mice, and only a few labeled fibers that did not extend far into the stomach wall were present in two of the P0 mice and the P3 mouse. Fibers that were labeled after vagotomy could be traced back to the proximal cut end of the vagal gastric branch, suggesting they were of vagal origin, but had not been cut during sectioning of the vagus. Additionally, a few labeled fibers in one E16.5 embryo resulted from DiI redistribution. These results demonstrate that the anterograde DiI nerve tracing method used in this experiment indeed labeled the vagal fibers innervating the stomach wall, without inadvertently staining other components of stomach wall innervation such as sympathetic afferents or efferents.

3.3 Experiment 3. Characterization of DiI-labeled axons and terminal specializations

Specimens ranging in age from E12.5 to P8 that were labeled with DiI crystal application, preserved in fixative containing EDTA, incubated for 2.5 – 3 wk (embryos) or 4–5 wk (neonates), and mounted in PBS resulted in labeling of axons and terminal specializations. These results show, as elaborated in detail below, that there were several stages in the formation of fiber bundles within the myenteric plexus, and initial appearance and early stages of formation of nerve terminal specializations.

3.3.1 Development of fiber bundle and axon distribution—Examination of DiI-labeled axons in the stomach wall revealed distinct patterns of vagal innervation at different developmental stages. Two factors varied as development progressed: (1) changes in the density and distribution of individual fibers and axon bundles and (2) the growth of the stomach. Some of the observations at each age examined are summarized below.

E12.5 Axon bundles forming the gastric branches extended from the esophagus toward the greater curvature, but did not reach the greater curvature even with extended incubation times that permitted continued DiI diffusion.

E13.5 The gastric branches approached the greater curvature. Both fiber bundles and individual axons were present forming a dense network throughout the stomach wall (Fig. 2A). Additionally, individual axons had begun to exit the myenteric plexus to enter the adjacent muscle and mucosal/submucosal layers. Moreover, from this age on, in parallel with the increasing axon innervation, as the stomach grew in size, the distance between fiber bundles and between individual axons increased (Fig. 2A–C).

E14.5–15.5 The gastric branches extended as far as the greater curvature. The axons extending out of the myenteric plexus into the adjacent muscle and mucosal/submucosal layers increased in number (Fig. 2B).

E16.5 Large vagal axon bundles were present throughout the stomach wall, including the forestomach, corpus, and antrum, and the fiber bundles in the corpus were more numerous and larger in diameter than those in the forestomach and antrum. Moreover, the bundles appeared to have completed their formation, exhibiting an adult-like distribution (Fig. 2C). Also at this age, the large axon bundles distributed many small bundles and individual axons that extended into the muscle and mucosal/submucosal layers of the stomach wall in patterns or formations comparable to those seen in P0 mice (e.g., mucosa/submucosa, Fig. 3F; muscle, Fig. 5A, B).

3.3.2 Development of nerve terminal specializations—Consistent with the assumption that labeled nerve terminals specializations would exhibit some of the unique characteristics of fully differentiated vagal terminals, such putative IMA, IGLE and efferent terminal precursors were first identified in small numbers in the majority of embryos studied at E16.5. These nerve terminal specializations continued to increase in number and become more similar to their mature forms as development progressed through P8. At P10 DiI applications were not successful in labeling sufficient numbers of axons and terminals throughout the stomach wall. This was probably a result of the increasing DiI diffusion distances required as nerve branches and organs grew in size over the course of development. At each age examined the degree of maturation of each putative ending type varied. The descriptions below focus on the predominant morphologies observed in each age range. Further, at all ages where putative IMA, IGLE and efferent terminal precursors were observed their distributions were similar to their mature distributions: IMAs developed predominantly in the forestomach with IMAs in the circular muscle focused near the lesser curvature and those in the longitudinal muscle near the greater curvature, whereas IGLEs and efferent terminals developed in all the major stomach compartments. Examples of the use of optical sectioning for distinguishing the distribution of neural elements in one tissue layer as opposed to those of another layer, including IMAs, IGLEs, and fibers innervating the mucosa/submucosa are illustrated in Figure 3.

E16.5 Putative efferent terminals were present at E16.5 throughout most of the stomach wall, identified by DiI-labeled fibers that encircled myenteric neurons. At this stage single or small numbers of encircled neurons were present within a myenteric ganglion (e.g. at P0, Fig. 4A, B, C).

E17.5 – P3 Putative efferent terminals increased in number dramatically between E17.5 and P3 and by this stage appeared similar to mature ones. They were present in large numbers and were clustered together as they surrounded a large proportion of neurons in many of the myenteric ganglia (examples at P0, Figs. 3E, 4D, E). Several efferent terminal fibers in close

proximity surrounded each neuron and thus individual fibers could not typically be distinguished. Moreover, efferent terminals were abundant in all stomach compartments.

P4 – P8 No significant increase in density or change in distribution or morphology of efferent terminals could be discerned after P3.

E16.5 – E17.5 At this stage putative precursors to IMAs and IGLEs were first detected. They were rare and appeared to be immature forms of the corresponding adult structures. Specifically, putative IGLE precursors consisted of laminar aggregates of fine terminal puncta in the focal plane between a myenteric ganglion and the adjacent smooth muscle layer much as in adults. However, they appeared to be immature in that the aggregates of terminal puncta were much smaller in area, and the terminal puncta within each aggregate were much less numerous and typically were not as tightly packed as in the mature form (e.g. at P0, Fig. 5B). At this stage of development, putative IMA precursors appeared as fine, singular, short, telodendria within one of the muscle layers and were oriented parallel to its muscle fibers. No bridging elements connecting parallel telodendria were apparent (example of candidates for initial IMA telodendria formation at P0 are shown in Fig. 5A). However, at these ages some potential IMA precursors may represent mature IMAs because in mature mice some are composed of only one or two telodendria, which around the time of birth are sufficiently immature as to be difficult to distinguish from axons.

P0, P1 and P2 From P0 – P2, the telodendria of some putative IMA precursors were increased in length and occasional bridging collateral branches were present (Figs. 3B, and 5C, E). Moreover, IMA precursors already exhibited the adult pattern. Similarly, some putative IGLE precursors were larger with more numerous and densely packed terminal puncta, which exhibited several different morphologies, including small growth cones, small circular or near circular structures, or elongated finger-like processes (Figs. 3D and 5B, D).

P3, P4 and P5 Putative IGLE and IMA precursors continued to mature as described for P0 – P2. Some putative IGLE precursors continued to increase in area and in density of terminal puncta, but not to the extent observed in adults. Similarly, some putative IMA precursors exhibited rectilinear telodendria of increased length, but they did not reach adult size or number of bridging elements.

P8 Putative IMA and IGLE precursors had developed morphology with characteristics approaching those of mature IMAs (e.g., Fig. 5E; some IMAs at P0 such as this one had a morphology similar to mature IMAs except that their telodendria were not full length yet) and IGLEs (e.g., 5F). In particular, for IMAs the telodendria were long, crossbridge fibers were observed more frequently, and multiple putative precursor IMAs occurred in close proximity to one another forming large fields of putative IMA precursors. IGLEs became larger and more distinct from the closely associated efferent labeling. Interestingly, IGLEs had not yet exhibited large increases in numbers to approach the densities present in adults.

3.4 Experiment 4. Adaptation of DiI labeling method to vagal innervation of the esophagus and intestine

Successful labeling of vagal fiber bundles, individual vagal fibers, and putative precursors of mature vagal nerve terminals was observed throughout the length of the thoracic and abdominal esophagus (e.g., 6A, B), or the proximal portion of the duodenum (approximately 1 cm or 5/6 of total duodenum length; e.g., Fig. 6C, D), whereas no labeling was detected in more distal compartments of the intestine. Moreover, in attempts to label the distal intestine, the DiI application sites along the celiac branches were too close to the intestine, and resulted in DiI spread to the intestine wall. Thus, although innervation of the intestine wall distal to the

duodenum was labeled, the source of this labeling could have been DiI at the application site, or at the sites of redistribution. Therefore, other DiI application sites or labeling strategies need to be explored for labeling vagal innervation of the intestine distal to the duodenum. Nevertheless, the method as developed here will be valuable for examining vagal innervation of a large portion of the duodenum wall, which is the region of the intestine that is most densely innervated by the vagus nerve (Berthoud et al., 1991;Berthoud et al., 1997;Fox et al., 2000;Wang and Powley, 2000).

4. Discussion

In the present study a method utilizing anterograde diffusion of DiI to label both afferent and efferent vagal projections to the mouse GI tract wall during embryonic and early postnatal stages of development was successfully established. This is a significant advance because it will make possible the characterization of the temporal and spatial pattern of the normal development of vagal innervation of the GI tract, and of perturbations in these patterns produced by pharmacological, surgical or genetic manipulations employed for investigation of the mechanisms that orchestrate vagal development. Examination of labeled innervation at ages this DiI method was practical to use (E12.5 - P8) provided information about the arrival of axons in the GI tract, the formation of myenteric plexus axon bundles, and the early differentiation of nerve terminal specializations, an important phase of vagal development.

4.1 Establishing a DiI anterograde tracing method

The method of labeling the pre- and postnatal vagal innervation of the murine GI tract with DiI was successfully established by incorporating into our initial protocol several modifications that had been developed in previous studies. The key modifications included: (1) Use of DiI crystals for tracer application to vagal nerve trunks and branches was more effective than DiI solution dried onto glass micropipette tips, (2) addition of 0.1% EDTA to the fixative improved the stability of DiI labeling of nerve elements, especially with long incubation durations, and (3) DiI label in vagal fibers and endings appeared to be more stable and clear when mounted in PBS as compared to 70% glycerol with 5% n-propyl gallate.

The first modification of the DiI protocol involved maximizing the amount or concentration of DiI inserted into the vagal nerve branches. DiI travels along axons by lateral diffusion through its lipid bilayer membrane (Godement et al., 1987). Therefore, the rate and distance DiI travels along these axons will depend in part on the concentration or amount of DiI introduced into a nerve as well as other factors, including duration of fixation prior to DiI application, temperature and fiber system (Hofmann and Bleckmann, 1999). Although an accurate, well-controlled dose-response experiment was not conducted here, three different doses of DiI were applied to the anterior vagal gastric branch, albeit two doses were in dried oil form and one in crystal form (largest dose), and DiI labeling of vagal stomach wall innervation increased with increasing amount of DiI applied.

The second important change made to our initial DiI protocol involved the addition of EDTA to the fixative. In the present study DiI labeling of vagal fibers appeared to become diffuse with long durations of tissue incubation, suggesting leakage of DiI from labeled vagal elements. A similar effect had also been observed with anterograde DiI tracing of vagal innervation of the esophagus in mouse embryos (Sang and Young, 1998) and in a study that involved DiI application to the optic nerve and vagal lobe in goldfish (Hofmann and Bleckmann, 1999). Hofmann and Bleckmann (1999) combined EDTA with reduced temperature to maintain the stability of DiI labeling during lengthy incubations, but it appeared that under the conditions in the present study EDTA alone was sufficient. Removal of calcium from the tissue and incubation solution by EDTA may have prevented membrane lipids from precipitating and free hydrophobic lipids from producing insoluble compounds that could have incorporated DiI and

then diffused through the cell plasma or extracellular space (Hofmann and Bleckmann, 1999).

The third critical modification to our DiI protocol involved mounting the tissue in PBS for imaging. Although 70% glycerol with 5% n-propyl gallate is often used for this purpose, the latter to reduce fading of fluorescence, in our tissue it appeared that the solubility of DiI in glycerol promoted DiI leakage out of labeled nerve elements, and thus contributed to the cloudiness of the DiI-labeled tissue and loss of specific labeling. In contrast, mounting specimens directly in PBS provided images in which distinct endings and fibers could be imaged.

4.2 Development of vagal gastric branches and myenteric fiber bundles

Using the DiI protocol developed here in the mouse we observed a similar pattern of development of vagal stomach wall innervation by the gastric branches and their derrivative axon bundles as previously reported by Boekelaar and Bloot (1986), employing acetyl cholinesterase *in toto* staining in the rat, and Xiang and Burnstock (2004), utilizing $P2X_3$ staining in the rat. The distribution of single fibers and axon bundles we observed is also consistent with the results of Swithers et al. (2002) as they reported the mature pattern to be present by P10 and we, similar to Boekelaar and Bloot (1986) found it to be established even earlier in development.

4.3 Early development of putative afferent and efferent nerve terminals

Vagal sensory axons first reach the gut by E12 and efferent (preganglionic) axons do so by E13 – E14 (Rinaman and Levitt, 1993), whereas potential precursors of mature afferent and efferent endings first became apparent at E16.5 in the present study. Further, putative efferent terminals developed at a faster rate than putative afferent endings and they increased in number at earlier ages: efferents increased in number significantly prior to P3, whereas afferents (e.g., IGLEs and IMAs) only began to increase in density around P3.

To our knowledge three previous investigations examined vagal nerve fibers and terminals within the developing gut, and in most instances our results are in agreement with their findings. In the first of these studies, Sang and Young (1998) used DiI in a similar manner to the present study, and reported that vagal axons were present in the myenteric plexus and ganglia in the esophageal muscle wall by E13, IGLE-like terminals were first observed in this tissue at E15, and they were more differentiated by E18. Embyronic day 15 is 1.5 d earlier than the age at which we first observed putative IGLE precursors in the stomach wall, a delay consistent with the rostral-to-caudal direction of maturation of nerve plexuses in the gut. In another study, anterograde labeling of stomach wall innervation with WGA-HRP in the rat revealed that at P10 differentiated IGLEs displayed an adult-like distribution and they were already present at densities similar to adults (Swithers et al., 2002). Although the distribution of differentiated IMAs was also similar to the mature pattern – largely restricted to the forestomach - they were much less dense than in adults. Consistent with these findings, at the oldest age we studied, P8, IGLEs and IMAs were close to achieving the differentiated forms previously described in adult rodents, and their distributions were similar to the adult (e.g., Berthoud and Powley, 1992;Neuhuber, 1987;Rodrigo et al., 1975;Wang and Powley, 2000). In the third study of developing vagal terminals, Xiang and Burnstock (2004) employed IHC detection of $P2X_3$ receptors in the rat and reported that IGLEs were first present at P1 and IMAs at P7, whereas we first observed putative precursors of these receptors at E16.5. The factor that probably contributed most to this age difference is that we included putative immature IMA and IGLE forms, whereas Xiang and Burnstock may have focused on terminals with a more mature appearance.

4.4 Limitations of anterograde DiI tracing of vagal innervation of the GI tract during development

One limitation of the method elaborated here is the restriction of its use to the middle portion of the period of vagal development (E12.5 to P8). Prior to E12.5, it was not feasible to apply DiI crystals because embryonic tissues were too small and fragile. After P8 it became increasingly difficult to adequately label sufficient numbers of axons and terminals throughout the target organ, probably the most significant limiting factor being the increasing DiI diffusion distances required as development progressed. However, it may be possible to identify IHC markers useful at ages prior to E12.5, and neural tracer methods used in adult rodents are feasible soon after P8. For example, IHC staining of the $P2X_3$ receptor has been used to label the gastric branches growing into the stomach wall as early as E12 (Xiang and Burnstock, 2004), and deleted in colorectal cancer (DCC) immunoreactivity has been observed within the vagal trunks running along the esophagus as they approached the stomach (Ratcliffe et al., 2006). Later in postnatal development, which may be a critical window for examining developmental events associated with weaning, Swithers et al. (2002) have successfully labeled vagal sensory innervation of the stomach wall using WGA-HRP injections into the rat nodose ganglion at P9 and we have similarly labeled vagal sensory innervation of the mouse upper GI tract as early as P12 (Fox, unpublished observations).

A second limitation of this method is that both efferent and afferent vagal axons are labeled and currently they cannot be distinguished. However, if the ratio of afferent:efferent axons is similar during development as in adults, with the majority of axons (>80%) being sensory (Berthoud and Powley, 1992;Neuhuber, 1987), then the effects of manipulations that affect large numbers of sensory axons should be detectable. Moreover, efferent and afferent terminals could typically be distinguished in our preparations by a combination of unique morphological features and unique locations within a GI organ and its specific tissue layers. Additionally, it should be noted that labeling both afferents and efferents can provide an advantage as the stability of labeling of one ending type can act as a control for specificity when manipulating the other type.

A third limitation is that although a large proportion of the vagal innervation appears to be labeled at all embryonic and postnatal stages for which our method was feasible (E12.5 – P8), it is not known what proportion of fibers present is stained with DiI, or whether this proportion is stable over the course of development. This precludes determination of absolute numbers of axons or terminals present at a given age as well as quantitative comparisons across different ages. However, comparisons made within age, for example, to assess the effects of genetic or pharmacological manipulations on development, should be informative regarding quantitative differences between mutants and wild-type controls, or drug treated and control mice. In support of this proposition, for each age examined, tissues with DiI-labeled vagal nerve fibers and terminals that met the criteria for inclusion in the present analyses exhibited consistent densities and distributions of labeled axons and endings.

Acknowledgements

We thank Dr. Qian Sang for helpful discussions and Jennifer Sturgis for technical assistance with the multi-photon confocal microscope of the Purdue University Cytometry Lab headed by Dr. J. Paul Robinson. Preliminary reports of the present findings were presented in abstract form at the annual meeting of the Society for Neuroscience (Murphy and Fox, 2003 and 2006). This manuscript was based in part on a dissertation submitted by M. Murphy in partial fulfillment of the requirements of the Master's degree. This work was supported by National Institutes of Health grant NS046716.

References

Berthoud HR, Carlson NR, Powley TL. Topography of efferent vagal innervation of the rat gastrointestinal tract. Am J Physiol 1991;260:R200–7. [PubMed: 1992820]

Berthoud HR, Patterson LM, Neumann F, Neuhuber WL. Distribution and structure of vagal afferent intraganglionic laminar endings (IGLEs) in the rat gastrointestinal tract. Anat Embryol 1997;195:183–91. [PubMed: 9045988]

Berthoud HR, Powley TL. Vagal afferent innervation of the rat fundic stomach: morphological characterization of the gastric tension receptor. J Comp Neurol 1992;319:261–76. [PubMed: 1522247]

Boekelaar AB, Bloot J. Some aspects of the development of the peripheral autonomic nervous system in the abdomen and the pelvis of the rat Preliminary results. Acta Histochem Suppl 1986;32:77–81. [PubMed: 3085163]

Castelucci P, Robbins HL, Furness JB. P2X(2) purine receptor immunoreactivity of intraganglionic laminar endings in the mouse gastrointestinal tract. Cell Tissue Res 2003;312:167–74. [PubMed: 12690440]

Elberger AJ, Honig MG. Double-labeling of tissue containing the carbocyanine dye DiI for immunocytochemistry. J Histochem Cytochem 1990;38:735–9. [PubMed: 2110209]

Fox EA, Phillips RJ, Martinson FA, Baronowsky EA, Powley TL. Vagal afferent innervation of smooth muscle in the stomach and duodenum of the mouse: Morphology and topography. J Comp Neurol 2000;428:558–76. [PubMed: 11074451]

Fritzsch B, Farinas I, Reichardt LF. Lack of neurotrophin 3 causes losses of both classes of spiral ganglion neurons in the cochlea in a region-specific fashion. J Neurosci 1997;17:6213–25. [PubMed: 9236232]

Fundin BT, Silos-Santiago I, Ernfors P, Fagan AM, Aldskogius H, DeChiara TM, Phillips HS, Barbacid M, Yancopoulos GD, Rice FL. Differential dependency of cutaneous mechanoreceptors on neurotrophins, trk receptors, and P75 LNGFR. Dev Biol 1997;190:94–116. [PubMed: 9331334]

Giloh H, Sedat JW. Fluorescence microscopy: reduced photobleaching of rhodamine and fluorescein protein conjugates by n-propyl gallate. Science 1982;217:1252–5. [PubMed: 7112126]

Godement P, Vanselow J, Thanos S, Bonhoeffer F. A study in developing visual systems with a new method of staining neurones and their processes in fixed tissue. Development 1987;101:697–713. [PubMed: 2460302]

Haworth K, Shu KK, Stokes A, Morris R, Stoker A. The expression of receptor tyrosine phosphatases is responsive to sciatic nerve crush. Mol Cell Neurosci 1998;12:93–104. [PubMed: 9790732]

Hayashi H, Ohsumi K, Fujiwara M, Mizuno N, Kanazawa I, Yajima H. Immunohistochemical studies on enteric substance P of extrinsic origin in the cat. J Auton Nerv Syst 1982;5:207–17. [PubMed: 6177727]

Hofmann MH, Bleckmann H. Effect of temperature and calcium on transneuronal diffusion of DiI in fixed brain preparations. J Neurosci Methods 1999;88:27–31. [PubMed: 10379576]

Holst MC, Kelly JB, Powley TL. Vagal preganglionic projections to the enteric nervous system characterized with Phaseolus vulgaris-leucoagglutinin. J Comp Neurol 1997;381:81–100. [PubMed: 9087421]

Honig MG, Hume RI. Fluorescent carbocyanine dyes allow living neurons of identified origin to be studied in long-term cultures. J Cell Biol 1986;103:171–87. [PubMed: 2424918]

Kirchgessner AL, Gershon MD. Identification of vagal efferent fibers and putative target neurons in the enteric nervous system of the rat. J Comp Neurol 1989;285:38–53. [PubMed: 2568999]

Krimm RF, Miller KK, Kitzman PH, Davis BM, Albers KM. Epithelial overexpression of BDNF or NT4 disrupts targeting of taste neurons that innervate the anterior tongue. Dev Biol 2001;232:508–21. [PubMed: 11401409]

Lukas JR, Aigner M, Denk M, Heinzl H, Burian M, Mayr R. Carbocyanine postmortem neuronal tracing. Influence of different parameters on tracing distance and combination with immunocytochemistry. J Histochem Cytochem 1998;46:901–10. [PubMed: 9671441]

Mirnics K, Koerber HR. Prenatal development of rat primary afferent fibers: I. Peripheral projections. J Comp Neurol 1995;355:589–600. [PubMed: 7636033]

Mitani S. Retarded gastrulation and altered subsequent development of neural tissues in heparin-injected Xenopus embryos. Development 1989;107:423–35. [PubMed: 2482166]

Neuhuber WL. Sensory vagal innervation of the rat esophagus and cardia: a light and electron microscopic anterograde tracing study. J Auton Nerv Syst 1987;20:243–55. [PubMed: 3693803]

Neuhuber WL, Kressel M, Dutsch M, Worl J, Berthoud HR. Relationships of IGLEs to enteric ganglia and neurons in the rat esophagus: Further indications of a mechanosensor-local effector role. Soc Neurosci Abstr 1995;21:1633.

Nosrat CA, Blomlof J, ElShamy WM, Ernfors P, Olson L. Lingual deficits in BDNF and NT3 mutant mice leading to gustatory and somatosensory disturbances, respectively. Development 1997;124:1333–42. [PubMed: 9118804]

Phillips RJ, Baronowsky EA, Powley TL. Afferent innervation of gastrointestinal tract smooth muscle by the hepatic branch of the vagus. J Comp Neurol 1997;384:248–70. [PubMed: 9215721]

Phillips RJ, Baronowsky EA, Powley TL. Long-term regeneration of abdominal vagus: efferents fail while afferents succeed. J Comp Neurol 2003;455:222–37. [PubMed: 12454987]

Raab M, Neuhuber WL. Number and distribution of intraganglionic laminar endings in the mouse esophagus as demonstrated with two different immunohistochemical markers. J Histochem Cytochem 2005;53:1023–31. [PubMed: 15923367]

Ratcliffe EM, Setru SU, Chen JJ, Li ZS, D'Autreaux F, Gershon MD. Netrin/DCC-mediated attraction of vagal sensory axons to the fetal mouse gut. J Comp Neurol 2006;498:567–80. [PubMed: 16917820]

Richards WG, Sugarbaker DJ. Neuronal control of esophageal function. Chest Surg Clin N Am 1995;5:157–71. [PubMed: 7743145]

Rinaman L, Levitt P. Establishment of vagal sensorimotor circuits during fetal development in rats. J Neurobiol 1993;24:641–59. [PubMed: 7686963]

Rodrigo J, de Felipe J, Robles-Chillida EM, Perez Anton JA, Mayo I, Gomez A. Sensory vagal nature and anatomical access paths to esophagus laminar nerve endings in myenteric ganglia. Determination by surgical degeneration methods. Acta Anat 1982;112:47–57. [PubMed: 7080798]

Rodrigo J, Hernandez J, Vidal MA, Pedrosa JA. Vegetative innervation of the esophagus. II. Intraganglionic laminar endings. Acta Anat 1975;92:79–100. [PubMed: 1163197]

Rontal DA, Echteler SM. Developmental segregation in the efferent projections to auditory hair cells in the gerbil. J Comp Neurol 2003;467:509–20. [PubMed: 14624485]

Sang Q, Young HM. The origin and development of the vagal and spinal innervation of the external muscle of the mouse esophagus. Brain Res 1998;809:253–68. [PubMed: 9853118]

Schafer MK, Eiden LE, Weihe E. Cholinergic neurons and terminal fields revealed by immunohistochemistry for the vesicular acetylcholine transporter. II. The peripheral nervous system. Neuroscience 1998;84:361–76. [PubMed: 9539210]

Swithers SE, Baronowsky E, Powley TL. Vagal intraganglionic laminar endings and intramuscular arrays mature at different rates in pre-weanling rat stomach. Auton Neurosci 2002;102:13–9. [PubMed: 12492131]

Travagli RA, Hermann GE, Browning KN, Rogers RC. Brainstem Circuits Regulating Gastric Function. Annu Rev Physiol 2006;68:279–305. [PubMed: 16460274]

Wang FB, Powley TL. Topographic inventories of vagal afferents in gastrointestinal muscle. J Comp Neurol 2000;421:302–24. [PubMed: 10813789]

Wang G, Scott SA. Independent development of sensory and motor innervation patterns in embryonic chick hindlimbs. Dev Biol 1999;208:324–36. [PubMed: 10191048]

Xiang Z, Burnstock G. Development of nerves expressing P2X3 receptors in the myenteric plexus of rat stomach. Histochem Cell Biol 2004;122:111–9. [PubMed: 15258768]

Zhang LL, Ashwell KW. The development of cranial nerve and visceral afferents to the nucleus of the solitary tract in the rat. Anat Embryol (Berl) 2001;204:135–51. [PubMed: 11556529]

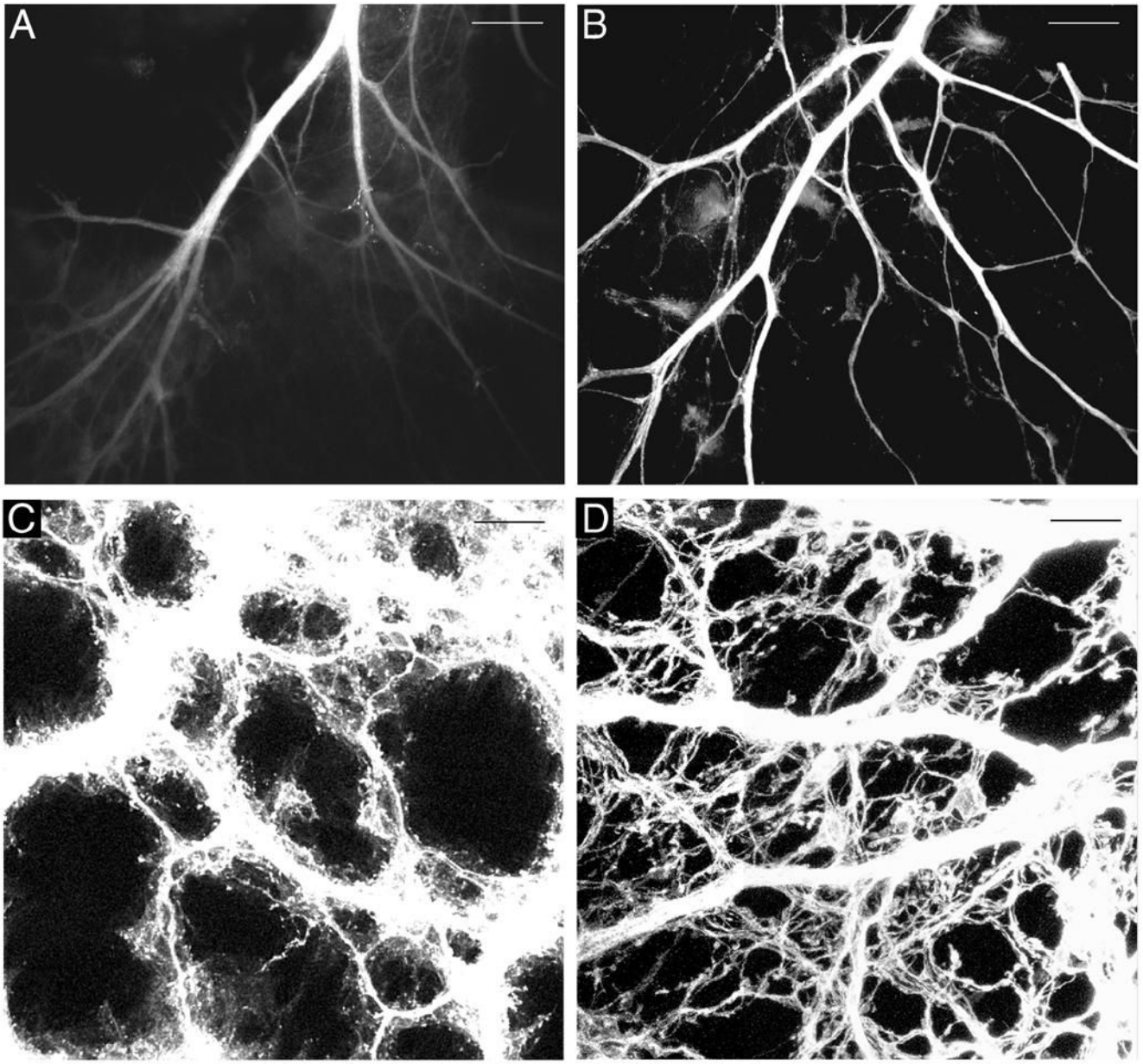

Fig 1.

DiI-labeled vagal anterior gastric branches adjacent to the lower esophageal sphincter at P0 (A,B) and axons in the forestomach at E16.5 with axon bundles overexposed to permit visualization of individual fibers (C,D). **A.** A fluorescence photomicrograph illustrating the reduced visibility of labeled fibers 6 wk after application of dried DiI oil (Experiment 1). **B.** A confocal image illustrating the more rapid DiI diffusion, more complete labeling, and absence of DiI leakage 2.5 wk after DiI crystal application and use of EDTA in the fixative. **C.** Confocal image of DiI-labeled tissue mounted in 70% glycerol, 5% n-propyl gallate. **D.** A confocal image of DiI-labeled axons from a comparable stomach region to that shown in C, but imaged from a stomach mounted in PBS. Scale bars = 200 μm (A,B), and 25 μm (C,D).

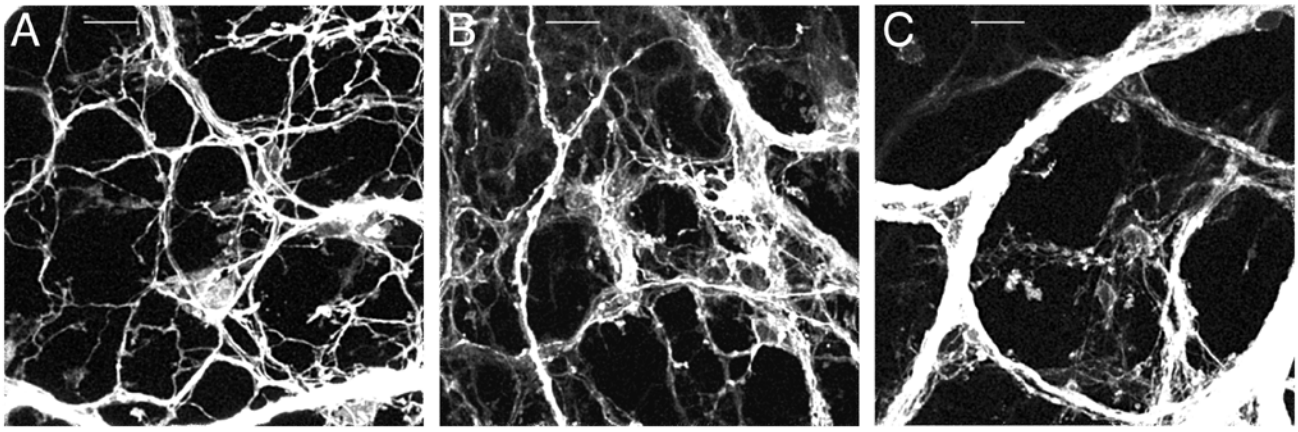

Fig 2.

Confocal images illustrating the development of vagal axon bundles in the myenteric plexus of the forestomach. **A.** At E13.5 a plexus-like pattern started to emerge and axon bundles were small in diameter. **B.** At E14.5 axon bundle diameters and distances between axon bundles increased, the latter due to stomach growth. **C.** By E16.5 axon bundle diameters and interbundle distances had again increased; a putative IGLE precursor is present in the center of this image. Scale bars = 25 μm (A,B,C).

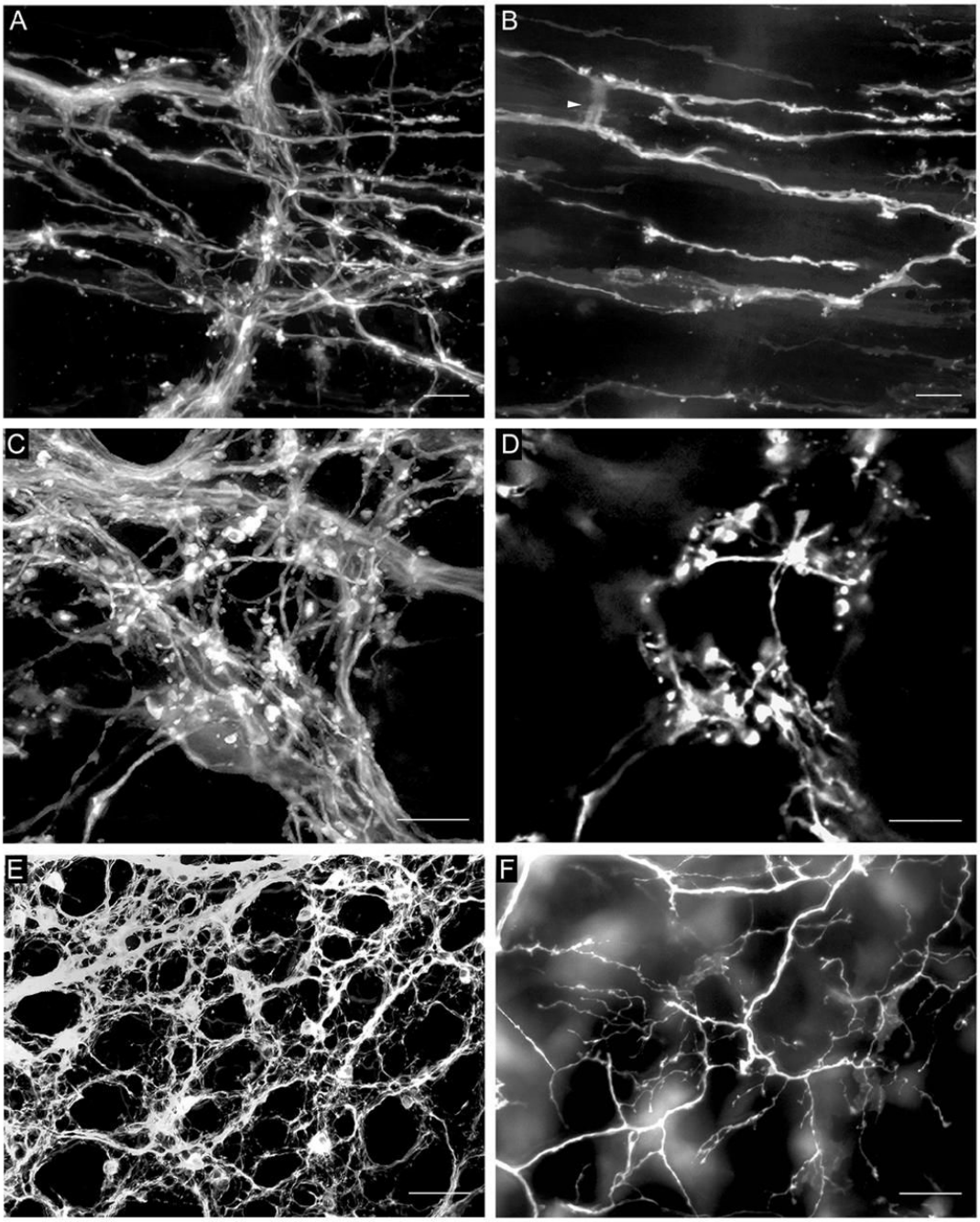

Fig 3.

A. DiI-labeled fibers in the myenteric plexus and putative IMA precursors in the underlying circular muscle. **B.** The same field as in A with imaging restricted to the circular muscle layer. DiI-labeled putative IMA precursors were present with two of their telodendria connected by a cross-bridge fiber (arrowhead). **C.** DiI-labeled fibers in the myenteric plexus and a putative IGLE precursor immediately below the plexus. **D.** The same field as in C with imaging restricted to the tissue plane immediately below the myenteric plexus, which contained the putative IGLE precursor. **E.** DiI-labeled fiber bundles and numerous putative efferent terminals in the myenteric plexus. **F.** The same field as in E with only the submucosa and mucosa imaged, which contained a network of fiber bundles, single axons and nerve terminals that originated

in the myenteric plexus. All images were from P0 mice. Scale bars = 10 μm (A–D) or 100 μm (E,F).

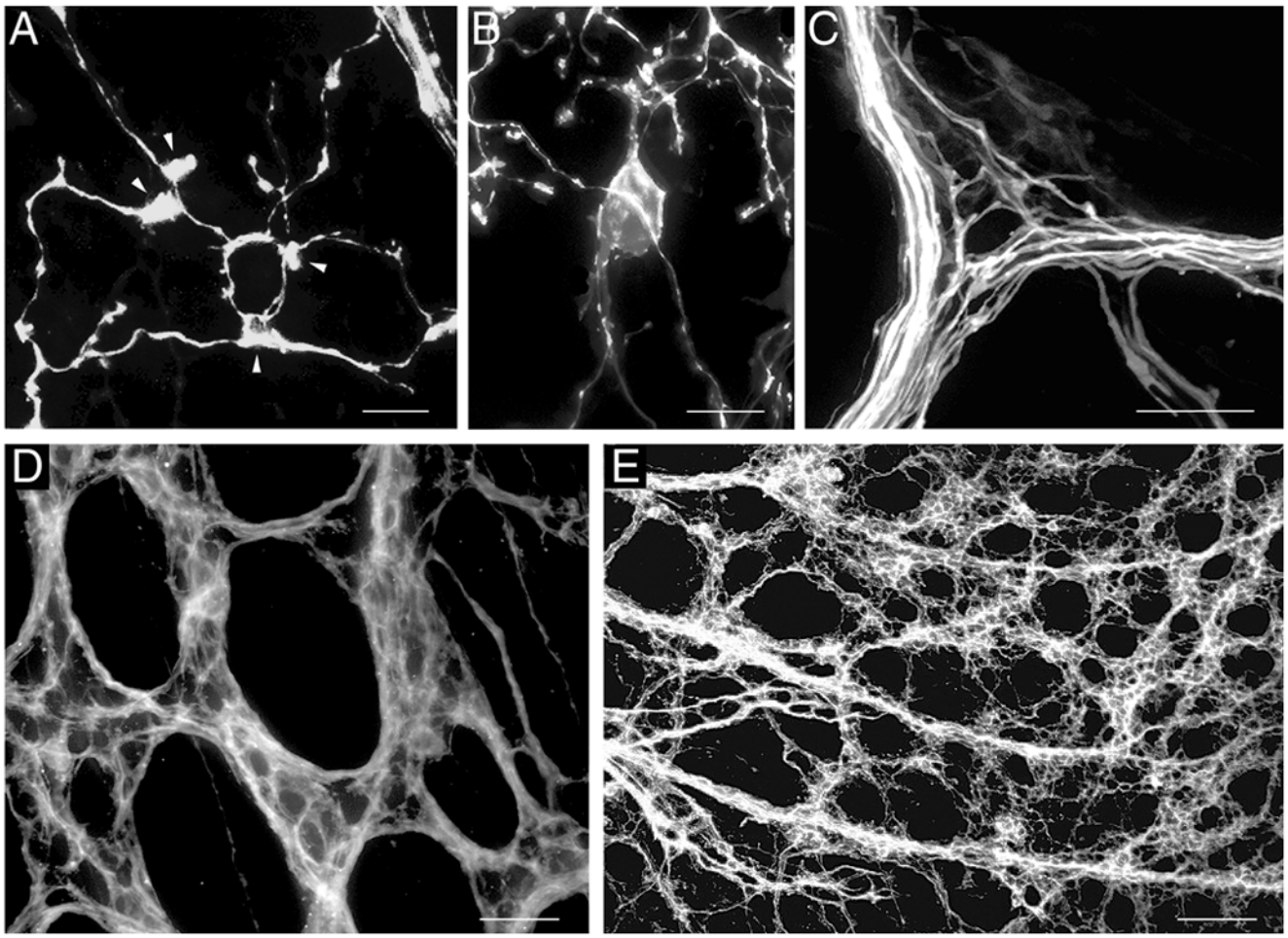

Fig 4.

A. A small number of fibers encircled a single myenteric neuron soma (not stained) to form immature putative efferent terminals in a P0 stomach wall. Several growth cone-like structures were present (e.g., arrowheads), two contributing to the efferent terminals. **B.** Immature putative efferent terminals appeared to partially encircle a myenteric neuron soma (at center of image) that was lightly stained with one dendrite extending upward and another downward in a P0 stomach wall. This neuronal staining was probably due to transfer of DiI from the labeled terminals to their target cell, which occurred rarely. **C.** A small number of immature putative efferent terminals appeared to be forming where an axon bundle branched in a P0 duodenum. Two myenteric neurons were completely encircled by a small number of fibers, and 2–3 more appeared to be partially encircled. **D.** An image of forestomach bundles and numerous putative efferent terminal precursors at P0. These appeared to be fairly mature with several fibers surrounding each myenteric neuron and bundled tightly so that individual DiI-labeled fibers could not typically be distinguished. **E.** An image of a field of axon bundles and numerous efferent terminals covering a large proportion of the forestomach at P0, illustrating the completeness of DiI labeling. Scale bars =10 μm (A,B,C), 20 μm (D), and 100 μm (E).

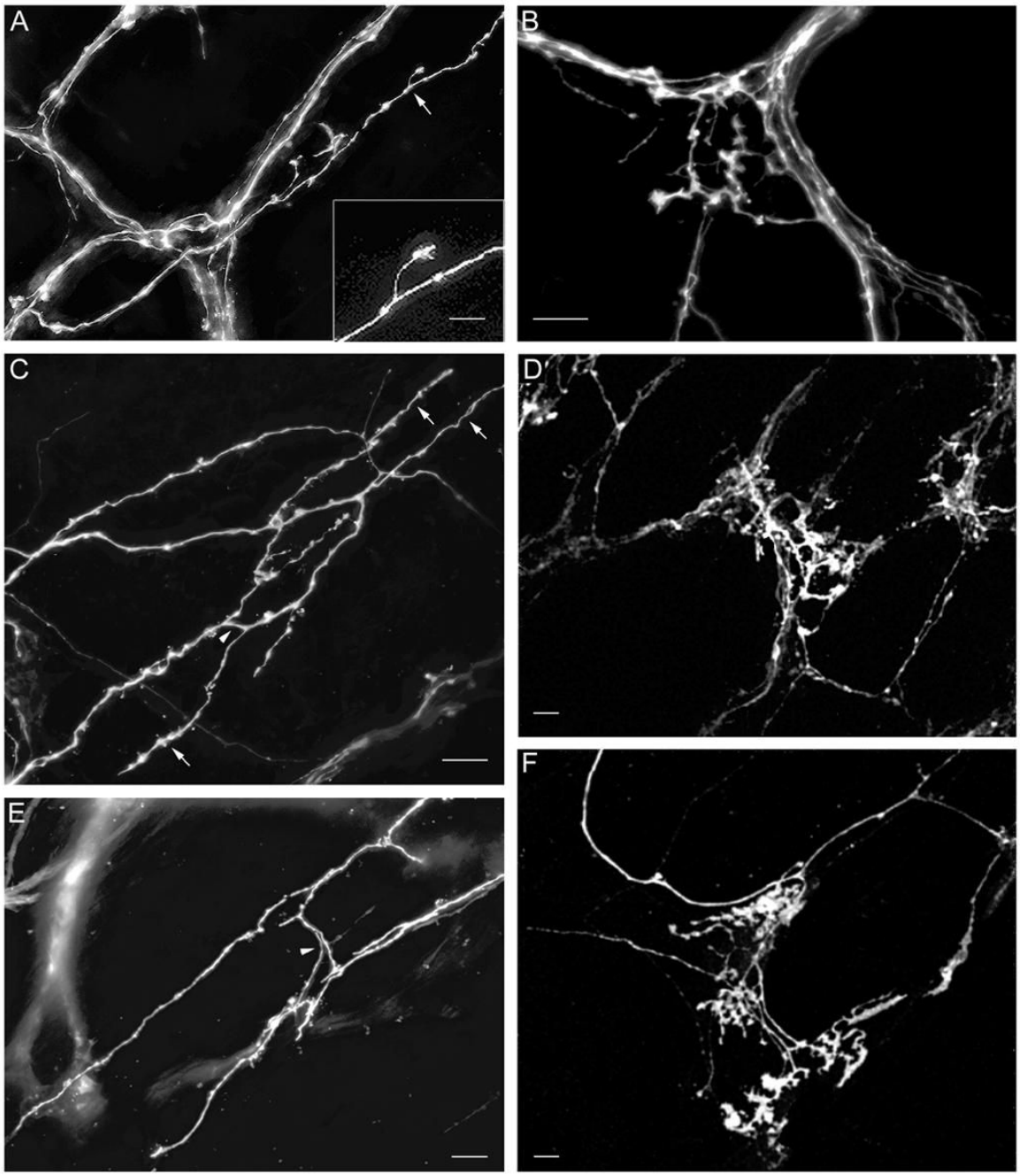

Fig 5.

Postnatal maturation of putative IMA (A, C, and E) and IGLE (B, D, and F) precursors. **A.** Initial formation of a putative IMA precursor at P0. The individual axon shown here exited the myenteric plexus in the lower left and continued diagonally to the upper right within the smooth muscle layer giving rise to short neurites – some with small growth cone-like structures - that might represent the initial formation of an IMA or its telodendria (arrow, neurite enlarged in inset). The other axons present are in the myenteric plexus. **B.** Cluster of growth cone-like terminals that may represent an initial stage of IGLE formation at P0. **C.** A putative IMA precursor at P0 at a later stage of maturation compared with that shown in A. Two axons arose from the myenteric plexus (at left out of field of view), entered the longitudinal muscle layer,

distributed additional axons and short rectilinear fibers forming IMA telodendria (e.g., arrows) that paralleled the muscle fibers, and an interconnecting crossbridge fiber (arrowhead). **D.** Putative IGLE precursor at P0 that may be more mature than the one illustrated in panel B. It exhibited more terminals and its morphology combined structural qualities of growth cones and terminal puncta. **E.** Putative IMA precursor at P0 in the circular muscle layer at a later stage of maturation as compared with that shown in C, in which the telodendria had lengthened and were connected by cross-bridge fibers (arrowhead)**. F.** A putative IGLE precursor at P8 at a stage of maturation beyond that shown in B and D. There were more terminal structures that were more densely packed, and were arranged in several groups with some lying below the plane of the myenteric plexus, and the others lying above it, suggesting some developing IGLEs "surround" a myenteric ganglion. Scale bars = 10 μm (A–F) and 25 μm (inset, A).

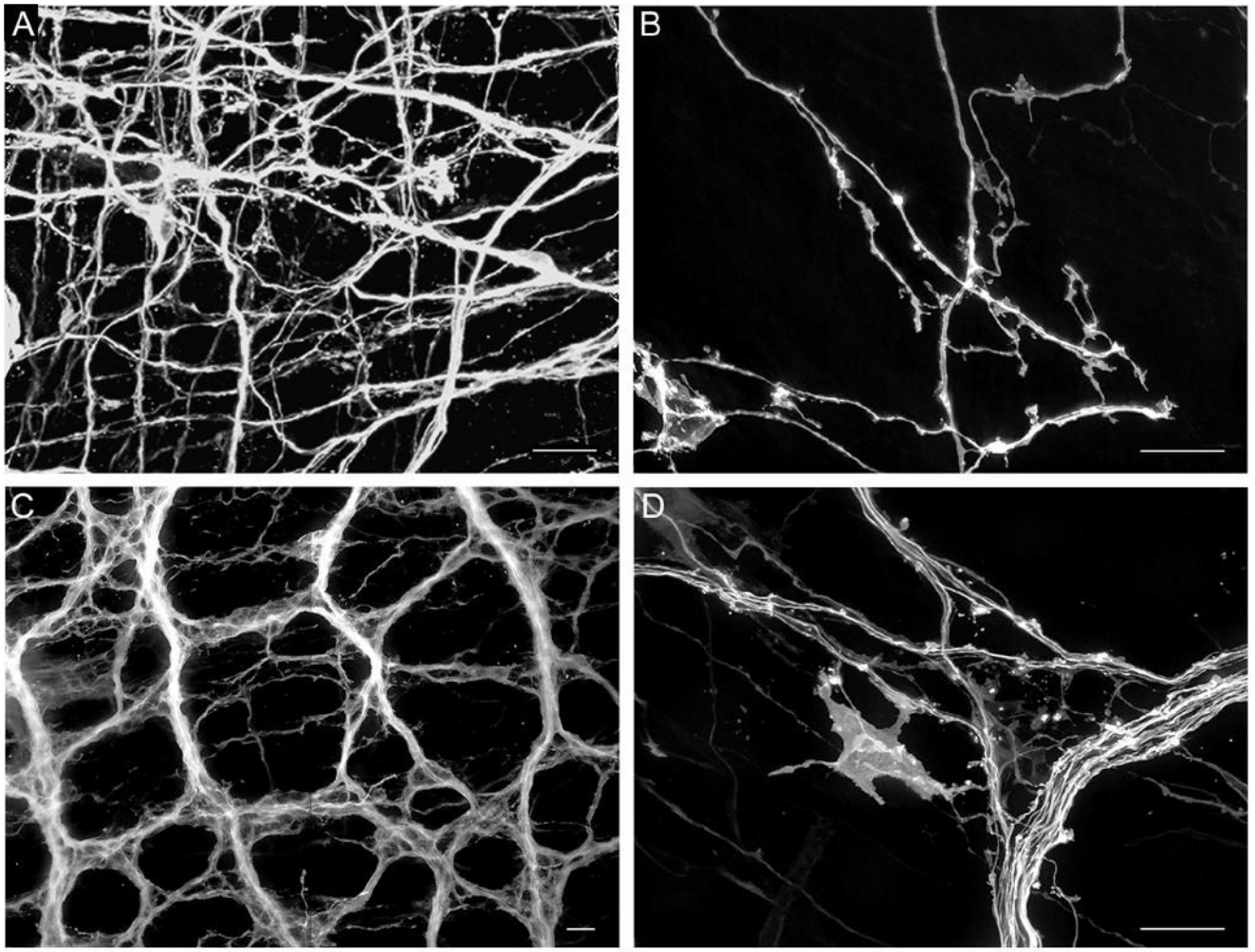

Fig 6.

A. Vagal myenteric network of the esophagus labeled at P0. **B.** Individual labeled fibers with small growth-cone like structures in the esophageal myenteric plexus at P0. **C.** DiI-labeled myenteric fiber bundles, axons and putative efferent terminals in the duodenum at P0. **D.** Labeled fiber bundle, single axons and large growth-cone like structure in the duodenal myenteric plexus at P0. Scale bars = 20 μm (A – D).